Eur Biophys J (2005) 34: 323–334
DOI 10.1007/s00249-004-0453-9

ARTICLE

Victor V. Skakun · Mark A. Hink · Anatoli V. Digris
Ruchira Engel · Eugene G. Novikov
Vladimir V. Apanasovich · Antonie J. W. G. Visser

Global analysis of fluorescence fluctuation data

Received: 14 September 2004 / Revised: 30 November 2004 / Accepted: 30 November 2004 / Published online: 12 February 2005

Abstract Over the last decade the number of applications of fluorescence correlation spectroscopy (FCS) has grown rapidly. Here we describe the development and application of a software package, FCS Data Processor, to analyse the acquired correlation curves. The algorithms combine strong analytical power with flexibility in use. It is possible to generate initial guesses, link and constrain fit parameters to improve the accuracy and speed of analysis. A global analysis approach, which is most effective in analysing autocorrelation curves determined from fluorescence fluctuations of complex biophysical systems, can also be implemented. The software contains a library of frequently used models that can be easily extended to include user-defined models. The use of the software is illustrated by analysis of different experimental fluorescence fluctuation data sets obtained with Rhodamine Green in aqueous solution and enhanced green fluorescent protein in vitro and in vivo.

Keywords Fluorescence correlation spectroscopy · Global analysis · Green fluorescent protein · Translational diffusion · Triplet state

Victor V. Skakun, Mark A. Hink and Anatoli V. Digris contributed equally to this work.

V. V. Skakun · A. V. Digris · V. V. Apanasovich
Department of Systems Analysis,
Belarusian State University,
Minsk, 220050, Belarus

M. A. Hink · R. Engel · A. J. W. G. Visser (✉)
MicroSpectroscopy Centre, Laboratory of Biochemistry,
Wageningen University, P.O. Box 8128,
6700 ET Wageningen, The Netherlands
E-mail: ton.visser@wur.nl
Fax: +31-317-484801

E. G. Novikov
Institut Curie, Section de Recherche,
Service Bioinformatique, 26 Rue d'Ulm,
75005 Paris, France

Abbreviations EGFP: Enhanced green fluorescent protein · FCS: Fluorescence correlation spectroscopy · FCCS: Fluorescence cross-correlation spectroscopy · GFP: Green fluorescent protein · PBS: Phosphate-buffered saline

Introduction

Fluorescence correlation spectroscopy (FCS) was introduced in the 1970s as a method for measuring molecular diffusion, reaction kinetics and flow of fluorescent particles (Magde et al. 1972, 1974, 1977; Elson and Magde 1974; Ehrenberg and Rigler 1974; Aragón and Pecora 1975, 1976). The underlying principles of FCS laid the foundation for a whole series of methods that are collectively referred to as fluorescence fluctuation spectroscopy. In FCS small spontaneous deviations from thermal equilibrium in an open system are reflected by fluctuations in the fluorescence intensity induced, for instance, by fluorescent molecules diffusing into and out of a well-defined observation volume generated by a focused laser beam. The first measurements, however, suffered from poor signal-to-noise ratios due to high background emission. It was not until the integration of confocal detection optics that the observation volume could be reduced to sub-femtoliter volumes, thereby reducing the background emission significantly (Qian and Elson 1991; Rigler et al. 1993). Moreover, the introduction of stable laser sources, highly efficient photon detectors, improved hardware correlators and high-quality microscopy optics greatly increased the sensitivity of FCS and subsequently increased the detection limit to the single-molecule level (Eigen and Rigler 1994; Rigler 1995; Maiti et al. 1997). In a typical experiment a focused laser beam continuously illuminates a fixed region within the sample. Although fluorescent particles throughout the excitation volume are excited, only the fluorescence from particles present in a limited observation volume is detected. Each time a

fluorescent molecule enters the observation volume a burst of fluorescence photons is detected. When diffusion is the only dynamic process causing intensity fluctuations, the duration of this photon burst reflects the time a particle needs to diffuse across the observation volume. Autocorrelation of the intensity fluctuations results in a curve that can be analysed to yield the average number of particles in the observation volume and the average diffusion time (or residence time). Alternatively, the amplitude of the emission bursts contains information about the molecular brightness of the particle, since bright particles will on average give rise to larger fluorescence bursts than dimmer molecules. The frequency of the fluorescence intensities can be plotted in a histogram of fluorescence intensities (Chen et al. 1999; Kask et al. 1999). Analysis of this photon distribution yields the molecular brightness and the number of the particles having that brightness. The molecular brightness can be defined as the number of detected fluorescence photons per molecule per second.

A brief summary of expressions for the autocorrelation function is given here. More extensive descriptions of the basic principles of FCS have been published elsewhere (Elson and Magde 1974; Thompson 1991; Rigler and Elson 2001). The normalised fluorescence fluctuation autocorrelation function $G(\tau)$ for the deviation of the signal $\delta I(t)$ from the average fluorescence intensity ($\delta I(t) \equiv I(t) - \langle I(t)\rangle$) is defined as

$$G(\tau) = 1 + \frac{\langle \delta I(t) \cdot \delta I(t+\tau)\rangle}{\langle I\rangle^2}. \tag{1}$$

The autocorrelation function describing j independent molecular species diffusing freely in a 3D-Gaussian-shaped observation volume ($V_{\mathrm{eff}} = \pi^{3/2}\omega_{xy}^2\omega_z$; ω_{xy} and ω_z are the lateral and axial radii, respectively) is

$$G(\tau) = 1 + \frac{1}{\langle N\rangle} \times \sum_j \frac{F_j}{\left(1+\frac{\tau}{\tau_{\mathrm{dif},j}}\right)\sqrt{1+\left(\frac{\omega_{xy}}{\omega_z}\right)^2\frac{\tau}{\tau_{\mathrm{dif},j}}}}, \tag{2}$$

where $j = 1, 2, 3,\ldots$ and $\sum_j F_j = 1$.

The lateral diffusion time τ_{dif} describes the residence time of a particle in the observation volume, which is related to the diffusion coefficient $\tau_{\mathrm{dif}} = \omega_{xy}^2/(4D_{\mathrm{tran}})$. The amplitude of the correlation function, $G(0)$, represents the average number of molecules $< N >$ found in the observation volume: $G(0) - 1 = 1/\langle N\rangle$.

In Eq. 2 it is assumed that the fluorescent brightness of a molecule is not changed during movement through the observation volume. However, an additional process commonly observed in autocorrelation analysis is intersystem crossing, the transition of a dye molecule from the first excited singlet state to the relatively long lived first excited triplet state. No fluorescence photons are emitted during the relaxation time to the ground state and the dye appears to be dark for a short interval (Widengren et al. 1995). It has been shown that intramolecular and intermolecular reactions that induce intensity fluctuations on a time scale much faster than motion-related fluctuations, thereby not altering the diffusion behaviour, can be taken into account by multiplying the motional term with one describing the reactions; therefore, $G_{\mathrm{total}}(\tau) = G_{\mathrm{motion}}(\tau) \cdot G_{\mathrm{kinetics}}(\tau)$ (Palmer and Thompson 1987; Widengren and Rigler 1998). The autocorrelation curves for a diffusing single species displaying intersystem crossing to the triplet state exhibit an additional shoulder on the microsecond time scale and are described by (Widengren et al. 1995):

$$G(\tau) = 1 + \frac{1}{\langle N\rangle} \times \frac{1 - T + T\mathrm{e}^{-\tau/\tau_{\mathrm{trip}}}}{(1-T)} \times \frac{1}{\left(1+\frac{\tau}{\tau_{\mathrm{dif}}}\right)\sqrt{1+\left(\frac{\omega_{xy}}{\omega_z}\right)^2\frac{\tau}{\tau_{\mathrm{dif}}}}}, \tag{3}$$

where T is the fraction of molecules in the triplet state and $1/\tau_{\mathrm{trip}}$ the corresponding triplet decay rate. If the observed system consists of multiple species with differences in molecular brightness η, the autocorrelation curve has to be adjusted by taking into account the molecular fraction Y and molecular brightness η of each species:

$$G(\tau) = 1 + \frac{1}{\langle N\rangle} \cdot \frac{1 - T + T\mathrm{e}^{-\tau/\tau_{\mathrm{trip}}}}{(1-T)} \sum_j \Phi_j \times \frac{1}{\left(1+\frac{\tau}{\tau_{\mathrm{dif},j}}\right)\sqrt{1+\left(\frac{\omega_{xy}}{\omega_z}\right)^2\frac{\tau}{\tau_{\mathrm{dif},j}}}}.$$

$$\text{with } \Phi_j = \frac{\left(\eta_j Y_j^2\right)}{\left(\sum_j \eta_j Y_j\right)^2}. \tag{4}$$

In Eq. 4 it is assumed that all species have the same triplet characteristics.

Besides measurements of local concentrations or diffusion times, FCS is capable of observing a whole range of other dynamic processes. Comprehensive reviews (Hess et al. 2002; Thompson et al. 2002; Bacia and Schwille 2003) and a book (Rigler and Elson 2001) dedicated to this technique clearly demonstrate its versatility. FCS measurements of molecules in solution include the observation of translational diffusion (Magde et al. 1974), rotational diffusion (Ehrenberg and Rigler 1974; Aragón and Pecora 1975, 1976), intersystem crossing (Widengren et al. 1995), chemical reactions (LaClair 1997), conformational dynamics of DNA hairpins (Bonnet et al. 1998), photobleaching (Eggeling et al. 2001), flavins and flavoproteins (Visser et al. 2001; Van den Berg et al. 2001), viscosity (Visser et al. 1999) and photodynamics of red fluorescent proteins (Schenk et al. 2004). FCS has also proved to be a suitable technique to detect nanoparticles and flowing particles (Akcakir et al. 2000; Kunst et al. 2002) and to study

membrane-mimetic systems (Bastiaens et al. 1994; Hink and Visser 1998; Hink et al. 1999; Korlach et al. 1999; Schwille et al. 1999a; Fradin et al. 2003). In addition, special studies have been addressed to investigate the flickering dynamics of variants of green fluorescent protein (GFP) (Haupts et al. 1998; Schwille et al. 2000; Heikal et al. 2000), the hybridisation of DNA and RNA sequences (Walter et al. 1996; Oehlenschläger et al. 1996), ligand–receptor interactions (Rauer et al. 1996) and the binding of single-chain antibodies to gram-negative bacteria (Hink et al. 2000). In recent years there have been an increasing number of publications concerning FCS in living cells (for a review, see Schwille 2001a). The first publications reported on the mobility of microinjected fluorospheres were by Berland et al. 1995 and Brock et al. 1998. The binding of substrates to the cell membrane of living cells (Rigler et al. 1999a; Pramanik et al. 1999; Boonen et al. 2000; Goedhart et al. 1999, 2000; Henriksson et al. 2001) or the diffusion of biological relevant molecules (Politz et al. 1998; Koopman et al. 1999; Cluzel et al. 2000) has also been described. Intracellular measurements demonstrated that FCS allows us to distinguish between different kinds of movement: active transport, 3D diffusion or restricted anomalous diffusion (Köhler et al. 2000; Wachsmuth et al. 2000; Schwille et al. 1999a). Furthermore, two-photon excitation has been implemented in FCS (Berland et al. 1995; Schwille et al. 1999a) and it was demonstrated that two-photon excitation can significantly improve the signal quality in turbid samples like plant cells or deep cell layers (Schwille et al. 1999b). From the reports on cellular FCS it has become clear that processes like cellular autofluorescence, photobleaching of the dye, cellular damage and reduced signal-to-noise ratios due to scattering and absorption can seriously interfere with the fluorescence fluctuation measurements in the living cell. These problems have been addressed in detail in relation with experiments in plant cells expressing different variants of GFP (Hink et al. 2003).

The application of FCS to study molecular interactions based upon differences in diffusion times is limited by the fact that the diffusion time is relatively insensitive to molecular weight. The diffusion coefficient of a spherical particle scales inversely to the hydrodynamic radius r_h of the particle according to the Stokes–Einstein relation $r_h = kT/(6\pi\eta_v D_{tran})$, where η_v is the viscosity, T the absolute temperature and k the Boltzmann constant. Assuming that r_h of the particle is proportional to the cube root of its molecular weight M, τ_{dif} can be rewritten as

$$\tau_{dif} \approx \frac{3\pi\omega_{xy}^2\eta_v}{2kT}\sqrt[3]{M}, \quad (5)$$

showing that τ_{dif} is proportional to the cube root of the molecular weight. Therefore, to study interaction between different molecules of almost equal sizes (as in the case of protein monomers and dimers) FCS will encounter problems in separating free diffusing molecules from molecular complexes. Meseth et al. (1999) have examined the resolving power of FCS to distinguish between differently sized particles. In the case of unchanged molecular brightness, the diffusion times of two species have to differ at least by a factor of 1.6, which corresponds to a minimum fourfold mass difference to distinguish the two species. Smaller mass differences may be retrieved from the autocorrelation traces but then detailed knowledge of, for instance, photophysical properties of each individual molecule is required. In most experimental systems and especially for measurements inside the living cell, these properties are hard to obtain. To overcome these limitations dual-colour fluorescence cross-correlation spectroscopy (FCCS) has been proposed (Eigen and Rigler 1994) and developed (Schwille et al. 1997, Schwille 2001b). In the last few years an increasing number of applications of dual-colour FCCS have been reported. These vary from enzyme kinetics (Kettling et al. 1998; Koltermann et al. 1998, Rarbach et al. 2001), nucleotide hybridisation (Schwille et al. 1997; Rigler et al. 1999b) and protein–DNA interactions (Rippe 2000) to the application of two-photon excitation (Heinze et al. 2000). Dual-colour FCCS applications in live cells have been reported recently (Bacia et al. 2002; Hink et al. 2003).

Given the wide variety of applications of fluorescence fluctuation spectroscopy it is necessary to focus attention on aspects of data analysis. In this paper we describe a software package that can be used for global analysis of correlation functions obtained by FCS. In global analysis several correlation functions are combined in one data set and are simultaneously fitted with certain parameters linked over the set, ensuring more reliable parameter recovery and thus a more consistent description of the underlying physical processes (Beechem et al. 1991; Beechem 1992; Verveer et al. 2000). Additionally, the quality of the fit and the performance of the optimisation method can be improved by fixing the parameters that are known a priori from independent experiments and by generating appropriate initial guesses for the parameters, for example, by the phase plane method (Novikov et al. 1999) adapted for the analysis of correlation functions. After giving a description of the structure of the program we present several examples of FCS measurements and subsequent numerical analyses to demonstrate the possibilities of the algorithms developed.

Materials and methods

Instrumental setup

Fluorescence fluctuation measurements were performed with a ConfoCor (Carl Zeiss & Evotec Biosystems, Germany), a commercial single-channel system based on a Zeiss Axiovert 135 inverted microscope with standard confocal epi-fluorescence microscope optics. All samples

were excited with the 488-nm line of an air-cooled argon-ion laser that was fibre-coupled to the back of the microscope. Inserting neutral-density filters in front of the laser output, we attenuated the intensity of the excitation light. Dichroic (LP500), excitation (488DF10) and emission (530DF60) mirrors mounted in filter sliders were employed to select the proper excitation wavelength and to separate the fluorescence from excitation light. A water-immersion C-apochromat 40× objective lens (N.A. 1.2) (Carl Zeiss, Germany) containing an adjustable ring to correct for slight refractive index mismatches focused the excitation light to a diffraction-limited spot and collected the fluorescence. Samples were stored in either an 8-well (Naglenunc, USA) or a 96-well plate (Whatman, UK) with a borosilicate bottom. To limit the size of the observation volume a size-adjustable and motor-controlled pinhole was placed in the image plane of the detection path. The diameter of the pinhole was optimised to a value of 40 μm where a maximal count rate per molecule was observed. An avalanche photodiode detector (SPCM-AQ, PerkinElmer, USA) was placed directly behind the pinhole. For FCS analysis the detector was coupled to a fast digital ALV5000E correlator card (ALV, Germany) that calculates the autocorrelation function in real time. The system was controlled by the Access 1.0.12 software (Carl Zeiss & Evotec Biosystems, Germany), which also allows the evaluation of single autocorrelation curves to a multicomponent 3D Brownian motion model fit including triplet kinetics (Eq. 3). To process raw data, the detector was coupled to a dual-channel 32-bit, PCI photon counting card (ISS, USA) (Eid et al. 2000) that was controlled by Vista 3.03 software (ISS, USA).

System calibration

The system was calibrated by optimising the position of the pinhole and the correction ring of the objective lens, using 100 nM Rhodamine Green (Molecular Probes, The Netherlands) in water. Optimal settings were reached when the highest molecular brightness η (kilohertz per molecule) was observed. The dimension of the confocal volume element is represented as the structure parameter $\mathrm{sp} = \omega_z/\omega_{xy}$. The structure parameter was obtained by fitting the autocorrelation curves of fluorophores with known diffusion coefficient to Eq. 3.

Samples

Rhodamine Green was dissolved in 100 mM phosphate-buffered saline (PBS), pH 7.5. Enhanced GFP (EGFP, F64L, S65T) was expressed and purified as described by Hink et al. (2003) and dissolved in 100 mM PBS, pH 7.5 containing 20% (w/v) sucrose. Buffer solutions at other pH were prepared by adding predetermined aliquots of 1 N HCl or NaOH. The final EGFP concentration in the experiments was 5 nM. *Dictyostelium discoideum* cells expressing EGFP or PH2-EGFP (S65T) were handled and cultured as described by Ruchira et al. (2004). Vegetative cells were incubated in phosphate buffer (17 mM, pH 6.5). Raw data traces were acquired over 90 s after positioning the detection volume at various positions of the cell, based on a fluorescence intensity scan along the optical (z-)axis or visual inspections.

Results and discussion

Description of software package

Most software packages delivered with FCS hardware are designed for controlling microscopes and therefore have quite limited capabilities for fitting correlation functions. In order to perform a detailed analysis of any measured FCS data set one needs an advanced software package that combines strong analytical power with simplicity of use. The FCS Data Processor (version 1.3) (for Windows 95/98/ME/NT 4.0/2000/XP) is such a package. During development of the FCS Data Processor software efforts were made to create analytical tools that provide quick and precise fit results for both simple and complex systems. To reach this goal a set of analysis algorithms and methods, consisting of previously known and some new self-developed routines, have been included in the software package.

Fluorescence autocorrelation curves of complex biophysical systems are most effectively analysed using the global analysis approach (Beechem et al. 1991), where several curves are fitted simultaneously. Often, the value of some of the parameters of the autocorrelation function measured for a set of samples under different experimental conditions can change with the conditions, while other parameters are unaffected. One example is the structure parameter ($\mathrm{sp} = \omega_z/\omega_{xy}$), which is unaffected by changing conditions and, hence, can be fixed in the analysis. Also, certain parameters that are expected to have the same value through all data sets can be linked. The fitting procedure keeps the values of the linked parameters equal to each other during the optimisation procedure. The advantage in the global analysis approach, compared with the fitting of individual autocorrelation functions, is that more information from the measurements is available for the optimisation routine, as many autocorrelation curves participate in the fit. At the same time the use of appropriate linking schemes can reduce the total number of parameters. The combined use of both elements will increase the accuracy of parameter estimation ensuring a more accurate representation of the model describing the system dynamics. The FCS Data Processor software allows adding and globally analysing a large number of data sets. Because the number of fit parameters is usually large, the interface implementation of the FCS Data Processor is designed to simplify the parameter management in the case of the use of global analysis. Parameters can be rapidly linked using the local menu commands enabling

multiple selection in the parameter lists and drag-and-drop operations.

It is well known that the accuracy of iterative fitting largely depends on the number of fit parameters and their initial guesses. The accuracy and speed of the analysis can be considerably increased by preliminary optimisation of the parameters. The FCS Data Processor provides the possibility to fix fit parameters that are known a priori from independent measurements. This improves the performance of the fit routine by decreasing the total number of parameters to be recovered. Also the possibility to set minimum and maximum limits for each unfixed parameter is implemented. This is useful in cases where the approximate range of values of a certain parameter is known. Setting parameter constraints also increases the speed of the optimisation routine and in many cases helps to avoid the trapping of the criterion function (χ^2 statistic) into a local minimum. In order to start the iterative fit procedure from the point closest to the global minimum of the criterion function, the FCS Data Processor software uses specially developed algorithms for generation of initial guesses of fit parameters. These algorithms are based on the phase plane method (Novikov et al. 1999) adapted for the analysis of correlation functions. In most cases generation of initial guesses makes it possible to perform the required analysis in a few seconds. This novel feature of the data evaluation package provides fast generation of most initial guesses for all fit parameters by clicking on only one interface button.

The accuracy of the analysis also depends on the weighting factors, calculated for each data point (Di Cera 1992). Using improper weighting factors or simply ignoring them may lead to parameter values that are not correct. Unfortunately, it is not possible to calculate directly the weighting factors from experimental correlation functions. Only approximations may be used (Koppel 1974; Wohland et al. 2001; Saffarian and Elson 2003). In the FCS Data Processor software the weighting factors are calculated from the raw data according to an algorithm proposed by Wohland et al. (2001). This algorithm divides the raw data into N segments, calculates N autocorrelations and finds corrected standard deviations from them.

The fit parameters are obtained by a global fitting procedure, based on the Marquardt–Levenberg nonlinear method of least squares (Marquardt 1963). The goodness of fit is judged by criteria such as the minimum χ^2 statistic and visual inspection of the residuals between experimental and fitted curves. An error estimation of the recovered parameters is performed by the exhaustive search method (Beechem et al. 1991). In this method the examined parameter is fixed at a number of values in a predetermined range, while other parameters are allowed to be adjusted to the minimum of the criterion function. Thus, the dependence of the criterion function values on the examined parameter is observed. The analysis stops when the calculated value of the criterion function becomes higher than the one obtained from the statistical F test (for that particular confidence level and number of degrees of freedom) (Bevington 1969). The confidence intervals in the FCS Data Processor can be calculated with any user-defined confidence probability.

The FCS Data Processor contains an easily extendable library of frequently used model functions that can be applied for analysis of fluorescence fluctuation data. The model library contains the ''pure-diffusion'' model that describes either the 2D- or the 3D-diffusion process for heterogeneous samples (Thompson 1991; Brock et al. 1998), the ''triplet-state'' model that, in addition to diffusion, also takes into account populating and depopulating of the triplet state (Widengren et al. 1995), the ''conformational'' model that is applicable when conformational changes take place in diffusing molecules (Edman et al. 1996) and the ''protonation'' model that represents the correlation function in the case of fluorescence fluctuations associated with proton association and dissociation kinetics (Haupts et al. 1998). The FCS Data Processor also contains a special ''custom'' model that allows easy creation of user-defined models that can be directly applied for fitting measured data. This feature opens a way for the researcher to create and test self-developed models with minimum extra effort. All contents of user-defined models, including the number and the default settings of fit parameters, model formula and an optional description of the model, can be stored in the database and easily loaded back when necessary.

Interface features

The FCS Data Processor consists of three modules, a user-interface, a measurement database and an analysis part, that can be further developed independently. Correlation functions are imported into the measurement database. Raw data stored in photon-delay mode during the measurements can be imported too. A data editor allows selecting, removing or changing the bin width of certain sections of the raw data trace, after which a ''corrected'' autocorrelation curve can be calculated. This opens the possibility to analyse small sections of the measured data trace in the case that the complete trace is disturbed by artefacts such as intensity drifts (Chen et al. 2002; Ruchira et al. 2004) or the presence of high-intensity bursts due to the presence of multilabelled or aggregated particles (van Craenenbroeck et al. 2001). The correlation curves are then loaded into the analysis module that fits the data according to one of the standard models describing 2D, 3D, anomalous diffusion or user-defined fitting models. Correlation curves can be simulated as well on the basis of any model function. Regularly used model and parameter settings can be stored in templates to accelerate the fitting handling.

The structure of the software package developed is presented in Fig. 1. The user interface has been developed based on the principles of a multidocument interface enabling the opening of several experiments

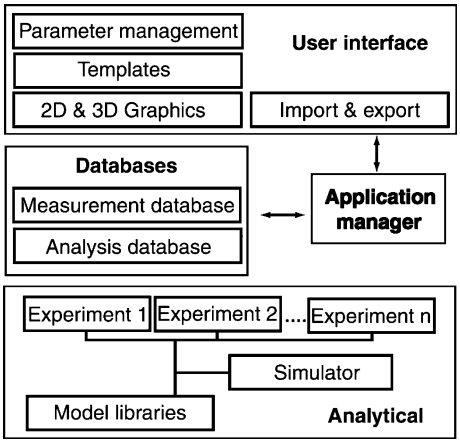

Fig. 1 Structure of the FCS Data Processor software. The software is built around an application manager that is connected to three different modules to be developed independently. The experimental and fitted data are managed by a database module. The analysis of the data takes place in the analysis module where the fluorescence autocorrelation curves can be fitted to standard or user-defined models. A user interface gives the possibility to control the experimental data, fit parameters and analysis schemes. The user can inspect the data via graphical presentations and export options allowing for storage of experimental and recovered correlation functions

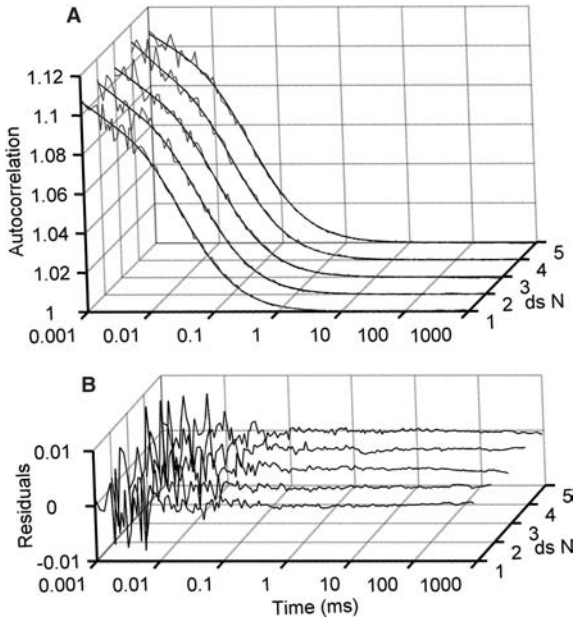

Fig. 2 **a** Fluorescence autocorrelation curves of Rhodamine Green in phosphate-buffered saline (*PBS*). Five experimental data sets (*grey lines*) were fitted globally (*black lines*) to the triplet-state model (Eq. 3) linking all fit parameters except the number of particles. **b** The residuals of the global fit

simultaneously and providing easy comparison of different fit trials. The following components are implemented in the user interface. The parameter management component simplifies the handling of a large number of parameters. Parameters can be rapidly linked using the local menu commands enabling multiple selections in the parameter list and drag-and-drop operations. Templates are available for quickly saving and restoring the most frequently used analysis schemes. Templates contain information about types, names and number of the models that should be used, parameter settings (such as the numerical value and minimum and maximum values), and information on linking of common parameters. Templates can be directly applied to the new data without any preliminary adjustment of the model and parameter configurations. The 2D and 3D graphical data representation is available for viewing measured and fitted data and the residuals. The 2D graphical windows can display either all curves simultaneously or any selected curve available from a particular experiment. These windows provide X–Y zoom and scroll possibilities. The 3D graphical component is designed to display all curves in three dimensions and to allow rotation of the complete image. The import and export component is used to load experimental data from the measurements database or to load analytical configurations from the analysis database. This latter database stores the results of the analysis: model configurations, parameter-linkage schemes, recovered values of the parameters and fitted correlation functions. In particular, it allows exporting of measured data and recovered correlation functions into ASCII files, to preview templates.

The global analysis technique is illustrated in this paper by analysis of different experimental data sets obtained with the ConfoCor instrument. The data refer to experiments performed with Rhodamine Green in aqueous solution and EGFP in vitro and in vivo.

Global analysis of fluorescence autocorrelation curves of Rhodamine Green

The autocorrelation curves of Rhodamine Green fluorescence intensity fluctuations were analysed using the triplet-state model (Eq. 3). To demonstrate the advantage of global analysis for recovery of more precise values of fit parameters, several autocorrelation curves were analysed separately and the confidence intervals for the diffusion time were determined. Afterwards the same correlation functions were analysed globally with linked diffusion times, triplet fraction, triplet lifetime and fixed structural parameter. The experimental and fitted curves are displayed in Fig. 2. The values and confidence intervals for the diffusion times and the triplet lifetimes obtained are presented in Table 1. As can be seen, the confidence interval obtained for both the diffusion and the triplet decay time is much narrower in the case of global fitting than in the case of separate fitting. It was also quite difficult to get a reliable value for the triplet fraction in the case of separate fitting. Without setting an upper limit it rises to 91.5% and the triplet lifetime becomes too short (approximately 0.19 μs). At this laser intensity an acceptable fit was obtained only after setting the upper limit for the triplet fraction to 20%. Therefore,

Table 1 Parameters retrieved by fitting five fluorescence correlation spectroscopy data curves of Rhodamine Green to the triplet-state model (Eq. 3)

Data set	τ_{dif} (μs)	Confidence interval for τ_{dif} (μs)	Confidence interval for τ_{dif} (%)	τ_{trip} (μs)	Confidence interval for τ_{trip} (μs)	Confidence interval for τ_{trip} (%)	χ^2 ($\times 10^6$)
1	32.97	30.30–36.19	8.10; 9.77	0.83	0.17–1.41	79.35; 69.80	3.0
2	32.39	29.76–35.55	8.12; 9.76	0.87	0.13–1.55	85.34; 77.70	3.5
3	33.43	31.05–36.35	7.12; 8.73	1.59	0.67–2.95	58.07; 85.76	2.6
4	33.92	31.08–36.89	8.37; 8.76	1.91	1.08–3.06	43.39; 60.70	2.8
5	31.23	30.25–32.40	3.14; 3.75	0.55	0.17–0.79	69.31; 43.75	1.8
Global set 1–5	32.63	31.53–33.86	3.37; 3.77	1.10	0.84–1.38	23.11; 25.75	2.7

To show the advantage of global analysis the data sets were fitted both separately and globally. The confidence intervals (at 97% level) for the diffusion time and triplet decay time indicate the standard deviation of these parameters. Each data set was acquired in 20 s using 110 μW of 488-nm excitation light

it is always preferable to analyse several measured data sets globally to get more reliable and precise values of estimated parameters.

Laser intensity dependence of Rhodamine Green fluorescence autocorrelation curves

It is well known that the time dependence of fluorescence fluctuations is affected by the applied laser intensity. At higher laser intensities a larger population of the molecules will be driven into the triplet state (Widengren et al. 1995). To study the dependence of the triplet-state population on the laser excitation intensity, fluorescence autocorrelation curves of Rhodamine Green have been determined using different neutral density filters to attenuate the laser intensity (Visser and Hink 1999). The autocorrelation functions were analysed using the model represented by Eq. 3. In Fig. 3a, a biphasic decay of the experimental autocorrelation curves can be observed. The slower decay has a constant amplitude and rate and represents diffusion-dependent fluctuations. The faster decay, which grows in amplitude when the laser intensity is increased, represents the relaxation of molecules in the (dark) triplet state. Since only the fraction of triplet-state molecules is dependent on the applied laser intensity, all fitting parameters except the triplet fraction, T, were globally linked. Figure 3b shows the fractional increase of triplet-state molecules when higher excitation intensities are used.

pH effects on EGFP fluorescence autocorrelation curves

Haupts et al. (1998) showed that the fluorescence intensity fluctuations observed for EGFP are not only caused by diffusion of the fluorescent protein but also depend on the pH of the aqueous solution. The pH dependence of the autocorrelation curves could be explained by two types of protonation processes. First, the intermolecular hydrogen-bonding network is in contact with the deprotonated form of Tyr66 of the chromophore in EGFP. Protonation of Tyr66 will significantly decrease the fluorescence quantum yield, since the protonated chromophore does not absorb light at the excitation wavelength of 488 nm. This effect is independent of the pH of the buffer and is referred to as internal protonation (Haupts et al. 1998). Second, the protonated Tyr66 can exchange its proton with the ones from the aqueous buffer surrounding the EGFP molecule. This latter effect is due to an external protonation process and can be studied by measuring autocorrelation curves of EGFP in aqueous solutions at different pH. We have repeated these experiments. The autocorrelation curves for EGFP measured at different pH were analysed globally using the model represented by Eq. 6, resulting in parameters describing the diffusion (τ_{dif}), internal protonation (amplitude P_{int} and characteristic time τ_{int}) and external protonation (amplitude P_{ext} and

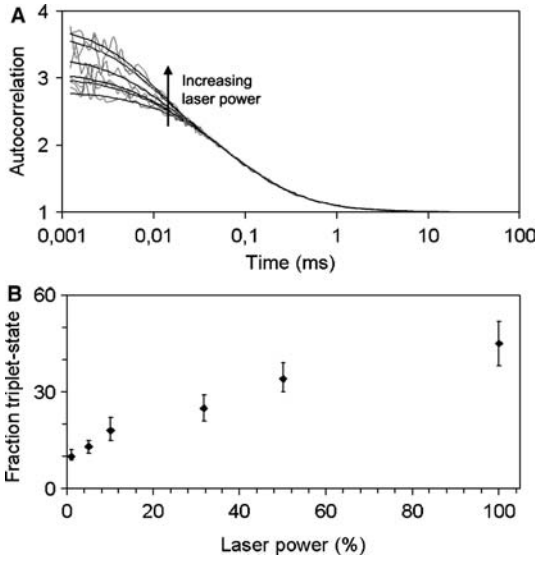

Fig. 3 Triplet-state dynamics of Rhodamine Green in PBS buffer. **a** The data sets were acquired in 20 s using 1.1 W of 488-nm excitation light attenuated by six different density filters. The curves were analysed using the triplet-state model (Eq. 3) with global linking of all parameters except the fraction of the triplet state. **b** The fraction of the triplet state (%) scales with the laser intensity. The confidence intervals at the 67% level are given for a global fit of 30 curves per set. The analysis resulted in $\tau_{dif} = 33$ (32–34) μs and $\tau_{trip} = 3.3$ (0.9–4.9) μs

characteristic time τ_{ext}) (for an extensive description of the model see Haupts et al. 1998).

$$G(\tau) = 1 + \frac{1}{\langle N \rangle} \times \left(1 + P_{ext} e^{-\tau/\tau_{ext}} + P_{int} e^{-\tau/\tau_{int}}\right) \times \frac{1}{\left(1 + \frac{\tau}{\tau_{dif}}\right)\sqrt{1 + \left(\frac{\omega_{xy}}{\omega_z}\right)^2 \frac{\tau}{\tau_{dif}}}} \quad (6)$$

For data sets obtained at pH 9–11 the pre-exponential factor for external protonation (P_{ext}) was fixed to 0, because this effect is negligible at high pH. The structural parameter was linked and fixed to the value obtained from the analysis of independently measured calibration data. The diffusion time, internal protonation time and pre-exponential factor for internal protonation are not dependent on the pH of the buffer and therefore were globally linked. The fitted autocorrelation curves and residuals are displayed in Fig. 4a and b and the values of the estimated parameters are presented in Table 2. The dependence of the pre-exponential factor and the external protonation time on pH, which is presented in Fig. 4c, is in good agreement with the results obtained by Haupts et al. (1998).

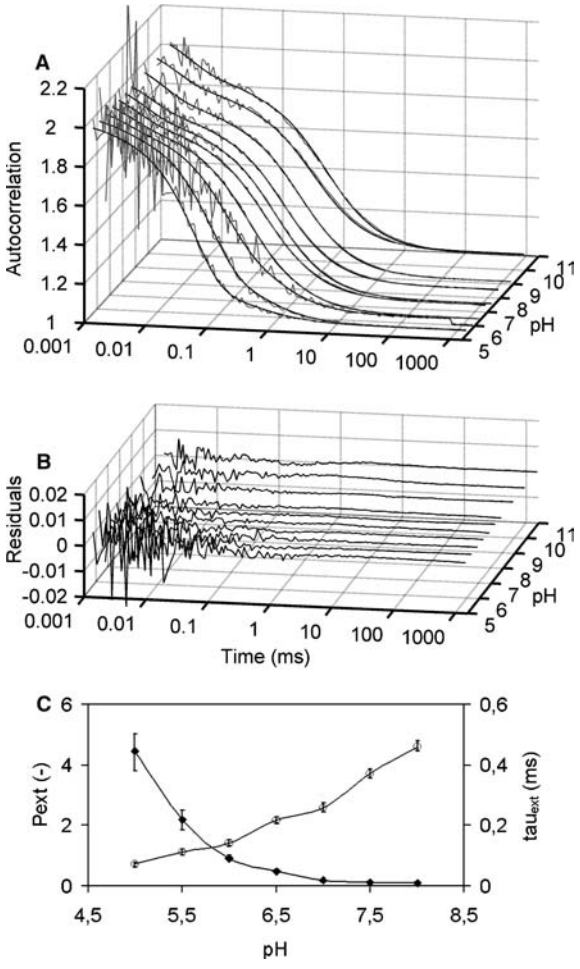

Fig. 4 Analysis of the autocorrelation curves of enhanced green fluorescent protein (*EGFP*) in buffers of different pH. **a** The data sets were fitted globally according a protonation-state model (Eq. 6) that yielded good quality fits as judged from the fit residuals in **b**. The autocorrelation curves were normalized at the origin. **c** The analysis resulted in parameters describing the internal and external protonation of the EGFP chromophore. The external protonation, i.e. the exchange of protons with the buffer, is dependent on the pH of the buffer. Precise analysis of the relation between P_{ext} (*filled diamonds*) and τ_{ext} (*open circles*) with pH provides insight into the chemical dynamics of this process

Fluorescence autocorrelation curves of EGFP fusion proteins in living cells

Nowadays the colour variants of GFP are widely used to fuse to proteins and follow the localisation and dynamics of these labeled molecules in the living cell. For example, one can follow the translocation of pleckstrin homology domain containing proteins from the cytoplasm to the plasma membrane (Ruchira et al. 2004). This process plays an important role in the chemotaxis mechanism of *Dictyostelium* cells (Parent and Devreotes 1999; Firtel and Chung 2000). The diffusion properties of free EGFP and PH2-EGFP, have been analysed using the FCS Data Processor. *Dictyostelium* cells move around continuously when incubated in a buffer. Cellular mobility can sometimes result in a drift of the observed fluorescence intensity, thereby introducing artefacts in the autocorrelation curve (Brock et al. 1999; Chen et al. 2002). An intensity trace obtained from a measurement of 90 s is shown in Fig. 5a. The drifts take place on a time scale of a few seconds and are probably due to cellular or intracellular movement. When the complete intensity trace is used for calculation of the autocorrelation curve, the artefact is clearly present on the long time scale (Fig. 5b, c). The curves were not successfully fitted with a 3D diffusion model, resulting in large fit-residuals and diffusion coefficients that are significantly smaller than the ones obtained in cells without fluorescence intensity drifts. In order to minimise the effect of the intensity drifts on the fitting parameters, the data editor of the software was used to analyse the data on time sections smaller than the typical time scale of the intensity drift. If the time sections are small the resulting signal-to-noise ratios will be low but can be overcome by analysing the data globally. When selecting the appropriate time sections a tradeoff must be made to minimise the duration of the selected segment but to maximise the signal-to-noise ratio. The six time sections, each approximately 10 s in size, were autocorrelated and globally analysed (Fig. 5d, e). The retrieved diffusion coefficients of around 22×10^{-12} m^2 s^{-1} (Table 3) are close to the values obtained in cells without fluorescence intensity drifts.

Concluding remarks

We have described global analysis techniques for analysis of fluorescence fluctuation data. The methodology is

Table 2 Analysis of the fluorescence autocorrelation curves of enhanced green fluorescent protein (*EGFP*) in buffers of different pH

τ_{int} (μs)		112
τ_{dif} (μs)		509
P_{int}		0.0549
pH	P_{ext}	τ_{ext} (μs)
5.0	4.457	0.073
5.5	2.195	0.112
6.0	0.919	0.142
6.5	0.486	0.217
7.0	0.193	0.258
7.5	0.120	0.372
8.0	0.098	0.461

The data sets were fitted globally according a protonation-state model (Eq. 6) resulting in parameters describing the diffusion (τ_{dif}) and the internal (P_{int}, τ_{int}) and external (P_{ext}, τ_{ext}) protonation

based on simultaneous analysis of multiple autocorrelation functions yielding internally consistent fitting parameters within finite confidence limits (obtained after a rigorous error analysis). The algorithms were tested for different experimental systems. First, we analysed a relatively simple system: a low concentration of the standard dye Rhodamine Green in aqueous solution. The model that best describes the experimental autocorrelation functions consists of two dynamic processes: triplet-state relaxation and (slower) diffusion. Global analysis linking of triplet-state lifetimes and diffusion times resulted in well-defined parameters. To demonstrate the potential of FCS in studying chemical reactions a more complex system was selected: EGFP in buffers of varying pH. The optimal model describing the experimental FCS data is one that includes two types of protonation reactions in addition to diffusion. Exploiting some prior knowledge of the internal protonation step in this system,we could precisely recover the parameters describing external protonation (proton exchange of chromophore with buffer) using global analysis. Finally, the most complex system consists of FCS measurements of EGFP in the confinement of a living cell. Here, the fluorescence intensity fluctuations often show an unpredictable pattern over time owing to (intra)cellular movements. By dissecting the fluorescence intensity trace into much smaller segments, global analysis of the short-time autocorrelation functions yielded realistic diffusion constants despite the lower signal-to-noise ratios of each individual curve. Although not demonstrated in this paper, the software tools can also be used to analyse FCCS data.

Summarising, we have shown that the FCS Data Processor with its strong analytical power and flexibility is a useful tool for FCS data analysis. The structure of the software package, which includes a data management system and an object-oriented modular analysis scheme, makes the software easily extendable and effective in use. In addition, the application of global analysis together with the generation of initial guesses

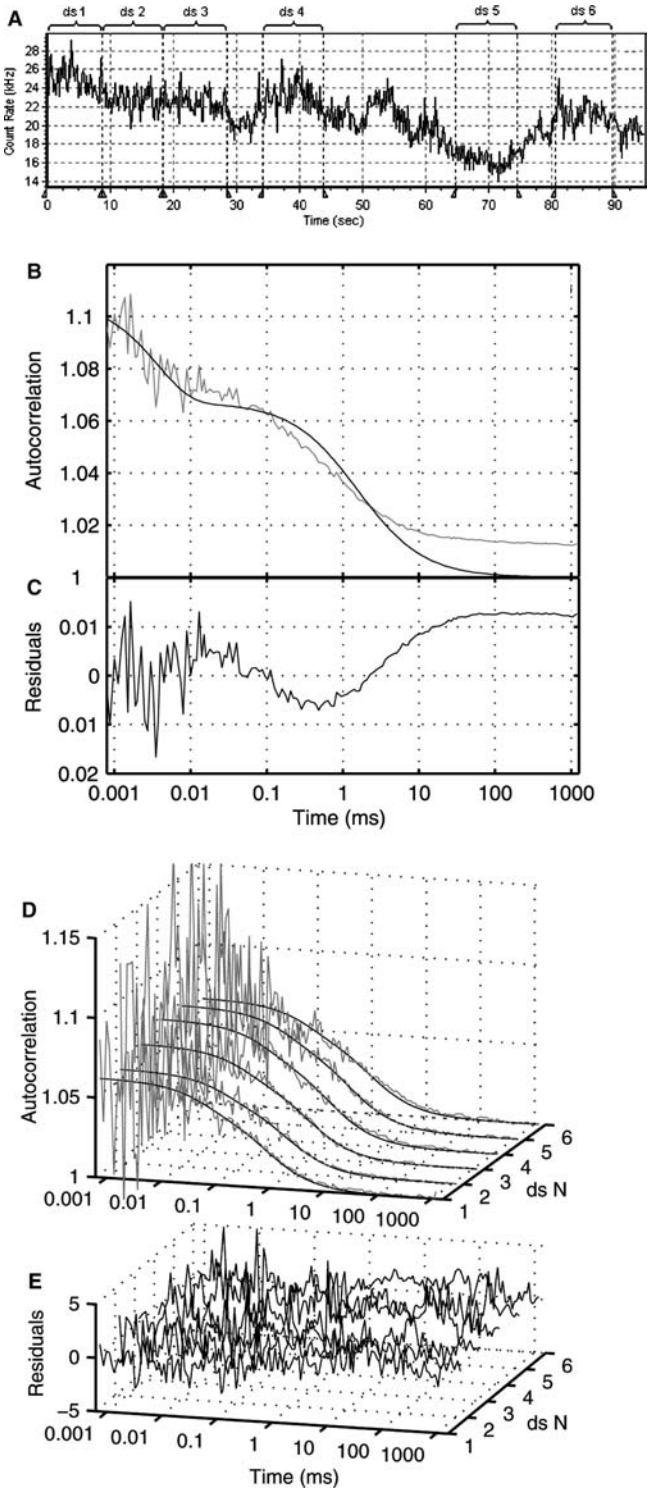

Fig. 5 **a** Fluorescence intensity of a *Dictyostelium* cell expressing PH2-EGFP. The data are binned to 200 ms. **b** The drift in the intensity as seen in **a** causes artefacts in the autocorrelation curve that cannot be fitted well to the triplet-state/diffusion model (Eq. 3) as judged from the fitting residuals in **c**. **d** In order to minimise the effect of the intensity drifts on the fitting parameters, six time sections, each approximately 10 s in size, were autocorrelated and globally analysed, resulting in significantly reduced residuals (**e**). The χ^2 value for fitting the whole trace was 167 and an average χ^2 of 1.558 was found for the globally fitted sections

Table 3 Diffusion coefficients of EGFP and PH2-EGFP expressed in immobilised *Dictyosteleum* cells

Sample	Fluorescence signal	$D\times10^{12}$ m^2 s^{-1} complete	$D\times10^{12}$ m^2 s^{-1} sectioned	Cells
EGFP	Stable	20 ± 4	20 ± 5	8
	Drifting	4 ± 4	17 ± 6	4
PH2-EGFP	Stable	22 ± 5	21 ± 6	4
	Drifting	5 ± 6	19 ± 7	6

The experimental FCS data sets were divided in two groups: intensity traces that have fluctuations less than 10% of the average intensity have been classified as "stable", otherwise the data set was classified as "drifting". The intensity traces were analysed completely (15 s) or sectioned in parts of 1 s. The (sub)traces were autocorrelated and fitted globally using the triplet-state model (Eq. 3)

increases the accuracy and speed of analysis, which can be further accelerated with the use of analysis templates.

More information on the FCS Data Processor can be obtained from info@sstcenter.com.

References

Akcakir O, Therrien J, Belomoin G, Barry N, Müller JD, Gratton E, Nayfeh M (2000) Detection of luminescent single ultra-small silicon nanoparticles using fluorescence fluctuation spectroscopy. Appl Phys Lett 76:1857–1859

Aragón SR, Pecora R (1975) Fluorescence correlation spectroscopy and Brownian rotational diffusion. Biopolymers 14:119–138

Aragón SR, Pecora R (1976) Fluorescence correlation spectroscopy as a probe of molecular dynamics. J Chem Phys 64:1791–1803

Bacia K, Schwille P (2003) A dynamic view of cellular processes by in vivo fluorescence auto- and cross-correlation spectroscopy. Methods 29:74–85

Bacia K, Majoul IV, Schwille P (2002) Probing the endocytic pathway in live cells using dual-color fluorescence cross-correlation analysis. Biophys J 83:1184–1193

Bastiaens PIH, Pap EHW, Widengren J, Rigler R, Visser AJWG (1994) Fluorescence methods to study lipid-protein association: the interaction of protein kinase C with lipid-loaded mixed micelles. J Fluoresc 4: 377–383

Beechem JM (1992) Global analysis of biochemical and biophysical data. Methods Enzymol 210:37–54

Beechem JM, Gratton E, Ameloot M, Knutson JR, Brand L (1991) The global analysis of fluorescence intensity and anisotropy decay data: second-generation theory and programs. In: Lakowicz JR (ed) Topics in fluorescence spectroscopy, vol 2. Plenum, New York, pp 241–305

Berland KM, So PTC, Gratton E (1995) Two-photon fluorescence correlation spectroscopy: method and application to the cellular environment. Biophys J 68:694–701

Bevington PR (1969) Data reduction and error analysis for the physical sciences. McGraw-Hill, New York

Bonnet G, Krichevsky O, Libchaber A (1998) Kinetics of conformational fluctuations in DNA hairpin-loops. Proc Natl Acad Sci USA 95:8602–8606

Boonen G, Pramanik A, Rigler R, Häberlein H (2000) Evidence for specific interactions between a kavain derivative and human cortical neurons measured by fluorescence correlation spectroscopy. Planta Med 66:7–10

Brock R, Hink MA, Jovin TM (1998) Fluorescence correlation microscopy of cells in the presence of autofluorescence. Biophys J 75:2547–2557

Brock R, Vamosi G, Vereb G, Jovin TM (1999) Rapid characterization of green fluorescent protein fusion proteins on the molecular and cellular level by fluorescence correlation microscopy. Proc Natl Acad Sci USA 96:10123–10128

Chen Y, Müller JD, So PTC, Gratton E (1999) The photon counting histogram in fluorescence fluctuation spectroscopy. Biophys J 77:553–567

Chen Y, Müller JD, Ruan Q, Gratton E (2002) Molecular brightness characterization of EGFP in vivo by fluorescence fluctuation spectroscopy. Biophys J 82:133–144

Cluzel P, Surette M, Leibler S (2000) An ultrasensitive bacterial motor revealed by monitoring signaling proteins in single cells. Science 287:1652–1655

Di Cera E (1992) Use of weighting functions in data fitting. Methods Enzymol 210:68–87

Edman L, Mets Ü, Rigler R (1996) Conformational transitions monitored for single molecules in solution. Proc Natl Acad Sci USA 93:6710–6715

Eggeling C, Berger S, Brand L, Fries JR, Schaffer J, Volkmer A, Seidel CAM (2001) Data registration and selective single-molecule analysis using multi-parameter fluorescence detection. J Biotechnol 86:163–180

Ehrenberg M, Rigler R (1974) Rotational Brownian motion and fluorescence intensity fluctuations. Chem Phys 4:390–401

Eid JS, Müller JD, Gratton E (2000) Data acquisition card for fluctuation correlation spectroscopy allowing full access to the detected photon sequence. Rev Sci Instrum 71:361–368

Eigen M, Rigler R (1994) Sorting single molecules: application to diagnostics and evolutionary biotechnology. Proc Natl Acad Sci USA 91:5740–5747

Elson EL, Magde D (1974) Fluorescence correlation spectroscopy I Conceptual basis and theory. Biopolymers 13:1–27

Firtel RA, Chung CY (2000) The molecular genetics of chemotaxis: sensing and responding to chemoattractant gradients. Bioessays 22:603–615

Fradin C, Abu-Arish A, Granek R, Elbaum M (2003) Fluorescence correlation spectroscopy close to a fluctuating membrane. Biophys J 84:2005–2020

Goedhart J, Röhrig H, Hink MA, van Hoek A, Visser AJWG, Bisseling T, Gadella Jr TWJ (1999) Nod factors integrate spontaneously in biomembranes and transfer rapidly between membranes and to root hairs, but transbilayer flip-flop does not occur. Biochemistry 38:10898–10907

Goedhart J, Hink MA, Visser AJWG, Bisseling T, Gadella TWJ (2000) In vivo fluorescence correlation microscopy (FCM) reveals accumulation and immobilization of Nod factors in root hair cell walls. Plant J 21:109–119

Haupts U, Maiti S, Schwille P, Webb WW (1998) Dynamics of fluorescence fluctuations in green fluorescent protein observed by fluorescence correlation spectroscopy. Proc Natl Acad Sci USA 95:573–578

Heikal AA, Hess ST, Baird GS, Tsien RY, Webb WW (2000) Molecular spectroscopy and dynamics of intrinsically fluorescent proteins: coral red (dsRed) and yellow (Citrine). Proc Natl Acad Sci USA 97:11996–12001

Heinze KG, Koltermann A, Schwille P (2000) Simultaneous two-photon excitation of distinct labels for dual-color fluorescence crosscorrelation analysis. Proc Natl Acad Sci USA 97:10377–10382

Henriksson M, Pramanik A, Shafqat J, Zhong Z, Tally M, Ekberg K, Wahren J, Rigler R, Johansson J, Jörnvall H (2001) Specific binding of proinsulin C-peptide to intact and to detergent-solubilized human skin fibroblasts. Biochem Biophys Res Commun 280:423–427

Hess ST, Huang S, Heikal AA, Webb WW (2002) Biological and chemical applications of fluorescence correlation spectroscopy: a review. Biochemistry 41:697–705

Hink MA, Visser AJWG (1998) Characterization of membrane mimetic systems with fluorescence correlation spectroscopy. In: Rettig W, Strehmel B, Schrader S (eds) Applied fluorescence in chemistry, biology and medicine. Springer, Berlin Heidelberg New York, pp 101–118

Hink MA, van Hoek A, Visser AJWG (1999) Dynamics of phospholipid molecules in micelles: characterization with fluorescence correlation spectroscopy and time-resolved fluorescence anisotropy. Langmuir 15:992–997

Hink MA, Griep RA, Borst JW, van Hoek A, Eppink MHM, Schots A, Visser AJWG (2000) Structural dynamics of green fluorescent protein alone and fused with a single chain Fv protein. J Biol Chem 275:17556–17560

Hink MA, Borst JW, Visser AJWG (2003) Fluorescence correlation spectroscopy of GFP fusion proteins in living plant cells. Methods Enzymol 361:93–112

Kask P, Palo K, Ullmann D, Gall K (1999) Fluorescence-intensity distribution analysis and its application in biomolecular detection technology. Proc Natl Acad Sci USA 96:13756–13761

Kettling U, Koltermann A, Schwille P, Eigen M (1998) Real-time enzyme kinetics monitored by dual-color fluorescence cross-correlation spectroscopy. Proc Natl Acad Sci USA 95:1416–1420

Köhler RH, Schwille P, Webb WW, Hanson MR (2000) Active protein transport through plastid tubules: velocity quantified by fluorescence correlation spectroscopy. J Cell Sci 113:3921–3930

Koltermann A, Kettling U, Bieschke J, Winkler T, Eigen M (1998) Rapid assay processing by integration of dual-color fluorescence cross-correlation spectroscopy: high-throughput screening for enzyme activity. Proc Natl Acad Sci USA 95:1421–1426

Koopman WJH, Hink MA, Visser AJWG, Roubos EW, Jenks BG (1999) Evidence that Ca^{2+} -waves in *Xenopus melanotropes* depend on calcium-induced calcium release: a fluorescence correlation microscopy and linescanning study. Cell Calcium 26:59–67

Koppel DE (1974) Statistical accuracy in fluorescence correlation spectroscopy. Phys Rev A 10:1938–1945

Korlach J, Schwille P, Webb W W, Feigenson G W (1999) Characterization of lipid bilayer phases by confocal microscopy and fluorescence correlation spectroscopy. Proc Natl Acad Sci USA 96:8461–8466

Kunst, BH, Schots A, Visser AJWG (2002) Detection of flowing fluorescent particles in a microcapillary using fluorescence correlation spectroscopy. Anal Chem 74:5350–5357

LaClair JJ (1997) Selective detection of the carbohydrate-bound state of concanvalin A at the single molecule level. J Amer Chem Soc 119:7676–7684

Magde D, Elson EL, Webb WW (1972) Thermodynamic fluctuations in a reacting system: measurement by fluorescence correlation spectroscopy. Phys Rev Lett 29:705–708

Magde D, Elson EL, Webb WW (1974) Fluorescence correlation spectroscopy. II. An experimental realization. Biopolymers 13:29–61

Magde D, Webb WW, Elson EL (1977) Fluorescence correlation spectroscopy III uniform translation and laminar flow. Biopolymers 17:377–412

Maiti S, Haupts U, Webb WW (1997) Fluorescence correlation spectroscopy: diagnostics for sparse molecules. Proc Natl Acad Sci USA 94:11753–11757

Marquardt DW (1963) An algorithm for least squares estimation of nonlinear parameters. J Soc Indust Appl Math 11:431–441

Meseth U, Wohland T, Rigler R, Vogel, H (1999) Resolution of fluorescence correlation measurements. Biophys J 76:1619–1631

Novikov EG, van Hoek A, Visser AJWG, Hofstraat JW (1999) Linear algorithms for stretched exponential decay analysis. Opt Commun 166:189–199

Oehlenschläger F, Schwille P, Eigen M (1996) Detection of HIV-1 RNA by nucleic acid sequence-based amplification combined with fluorescence correlation spectroscopy. Proc Natl Acad Sci USA 93:12811–12816

Palmer AG, Thompson NL (1987) Molecular aggregation characterized by high order autocorrelation in fluorescence correlation spectroscopy. Biophys J 52:257–270

Parent CA, Devreotes PN (1999) A cell's sense of direction. Science 284:765–770

Politz JC, Brown ES, Wolf DE, Pederson T (1998) Intranuclear diffusion and hybridisation state of oligonucleotides measured by fluorescence correlation spectroscopy in living cells. Proc Natl Acad Sci USA 95:6043–6048

Pramanik A, Juréus A, Langel Ü, Bartfai T, Rigler R (1999) Galanin receptor binding studies in the membranes of cultured cells measured by fluorescence correlation spectroscopy. Biomed Chromatogr 13:119–120

Qian H, Elson EL (1991) Analysis of confocal laser-microscope optics for 3-D fluorescence correlation spectroscopy. Appl Opt 30:1185–1195

Rarbach M, Kettling U, Koltermann K, Eigen M (2001) Dual color fluorescence cross-correlation spectroscopy for monitoring the kinetics of enzyme-catalyzed reactions. Methods 24:104–116

Rauer B, Neumann E, Widengren J, Rigler R (1996) Fluorescence correlation spectroscopy of the interaction kinetics of tetramethylrhodamin α-bungarotoxin with Torpedo calnifornica acetylcholine receptor. Biophys Chem 58:3–12

Rigler R (1995) Fluorescence correlations, single molecule detection and large number screening, applications in biotechnology. J Biotechnol 41:177–186

Rigler R and Elson EL (eds) (2001) Fluorescence correlation spectroscopy, theory and applications. Springer, Berlin Heidelberg New York

Rigler R, Mets Ü, Widengren J, Kask P (1993) Fluorescence correlation spectroscopy with high count rates and low background, analysis of translational diffusion. Eur Biophys J 22:169–175

Rigler R, Pramanik A, Jonasson P, Kratz G, Jansson OT, Nygren PÅ, Ståhl S, Ekberg K, Johansson BL, Uhlén S, Uhlén M, Jörnvall H, Wahren J (1999a) Specific binding of proinsulin C-peptide to human cell membranes. Proc Natl Acad Sci USA 96:13318–13323

Rigler R, Földes-Papp Z, Meyer-Almes FJ, Sammet C, Volcker M, Schnetz A (1999b) Fluorescence cross-correlation: a new concept for polymerase chain reaction. J Biotechnol 63:97–109

Rippe K (2000) Simultaneous binding of two DNA duplexes to the NtrC-enhancer complex studied by two-color fluorescence cross-correlation spectroscopy. Biochemistry 39:2131–2139

Ruchira, Hink MA, Bosgraaf L, Van Haastert PJM, Visser AJWG (2004) Pleckstrin homology domain diffusion in *Dictyostelium* cytoplasm studied using fluorescence correlation spectroscopy. J Biol Chem 279:10013–10019

Saffarian S, Elson EL (2003) Statistical analysis of fluorescence correlation spectroscopy: the standard deviation and bias. Biophys J 84:2030–2042

Schenk A, Ivanchenko S, Röcker C, Wiedenmann J, Nienhaus GU (2004) Photodynamics of red fluorescent proteins studied by fluorescence correlation spectroscopy. Biophys J 86: 384–394

Schwille P (2001a) Fluorescence correlation spectroscopy and its potential for intracellular applications. Cell Biochem Biophys 34:383–408

Schwille P (2001b) Cross-correlation analysis in FCS. In: Rigler R and Elson EL (eds) Fluorescence correlation spectroscopy. Theory and applications. Springer, Berlin Heidelberg New York, pp 360–378

Schwille P, Meyer-Almes FJ, Rigler R (1997) Dual-color fluorescence cross-correlation spectroscopy for multicomponent diffusional analysis in solution. Biophys J 72:1878–1886

Schwille P, Korlach J, Webb WW (1999a) Fluorescence correlation spectroscopy with single molecule sensitivity on cell and model membranes. Cytometry 36:176–182

Schwille P, Haupts U, Maiti S, Webb WW (1999b) Molecular dynamics in living cells observed by fluorescence correlation spectroscopy with one- and two-photon excitation. Biophys J 77:2251–2265

Schwille P, Kummer S, Heikal AA, Moerner WE, Webb WW (2000) Fluorescence correlation spectroscopy reveals fast optical excitation-driven intramolecular dynamics of yellow fluorescent proteins excitation. Proc Natl Acad Sci USA 97:151–156

Thompson NL (1991) Fluorescence correlation spectroscopy. In: Lakowicz JR (ed) Topics in fluorescence spectroscopy. Plenum, New York, pp 337–378

Thompson NL, Lieto AM, Allen NW (2002) Recent advances in fluorescence correlation spectroscopy. Curr Opinion Struct Biol 12:634–641

Van Craenenbroeck E, Vercammen J, Matthys G, Beirlent J, Marot C, Hoebeke J, Strobbe R, Engelborghs Y (2001) Heuristic statistical analysis of fluorescence fluctuation data with bright spikes: application to ligand binding to the human serotonin receptor expressed in *Escherichia coli* cells. Biol Chem 382:355–361

Van den Berg PAW, Widengren J, Hink MA, Rigler R, Visser AJWG (2001) Fluorescence correlation spectroscopy of flavins and flavoenzymes: photochemical and photophysical aspects. Spectrochim Acta 57A:2135–2144

Verveer PJ, Squire A, Bastiaens PIH (2000) Global analysis of fluorescence lifetime imaging microscopy data. Biophys J 84:2127–2137

Visser NV, Hink MA, Van Hoek A, Visser AJWG (1999) Comparison between fluorescence correlation spectroscopy and time-resolved fluorescence anisotropy as illustrated with a fluorescent dextran conjugate. J Fluoresc 9:251–255

Visser AJWG, Hink MA (1999) New perspectives of fluorescence correlation spectroscopy. J Fluoresc 9:81–87

Visser AJWG, Van den Berg PAW, Hink MA, Petushkov VN (2001) Fluorescence correlation spectroscopy of flavins and flavoproteins. In: Rigler R, Elson EL (eds) Fluorescence correlation spectroscopy, theory and applications. Springer, Berlin Heidelberg New York, pp 9–24

Wachsmuth M, Waldeck W, Langowski J (2000) Anomalous diffusion of fluorescent probes inside living cell nuclei investigated by spatially-resolved fluorescence correlation spectroscopy. J Mol Biol 298:677–689

Walter NS, Schwille P, Eigen M (1996) Fluorescence correlation analysis of probe diffusion simplifies quantitative pathogen detection by PCR. Proc Natl Acad Sci USA 93:12805–12810

Widengren J, Rigler R (1998) Fluorescence correlation spectroscopy as a tool to investigate chemical reactions in solutions and on cell surfaces. Cell Mol Biol 44:857–879

Widengren J, Mets Ü, Rigler R (1995) Fluorescence correlation spectroscopy of triplet states in solution: a theoretical and experimental study. J Phys Chem 99:13368–13379

Wohland T, Rigler R, Vogel H (2001) The standard deviation in fluorescence correlation spectroscopy. Biophys J 80:2987–2999